

Amphiphilic Egg-Derived Carbon Dots: Rapid Plasma Fabrication, Pyrolysis Process, and Multicolor Printing Patterns**

Jing Wang, Cai-Feng Wang, and Su Chen*

Carbon-based photoluminescent nanoparticles have recently received increased interest, owing to their favorable optical properties along with their biocompatibility and low toxicity.^[1] Such nascent nanomaterials, the so-called carbon dots (CDs or C-dots), are a promising alternative to more toxic metal-based semiconductor quantum dots (QDs) for applications such as bioimaging.^[2] Recent advances in the synthesis of CDs^[3] allow them to be formed from fine carbon structures (like graphene^[4] and multi-wall carbon nanotubes^[5]) by top-down methods, or from chemical precursors (like ammonium citrate^[6] and ethylenediaminetetraacetic acid^[7]) by bottom-up approaches. Typically, these CDs require surface oxidation and/or further passivation to emit fluorescence, which also makes them hydrophilic.^[8] Alternatively, some one-step strategies to fabricate surface-passivated CDs have also been shown.^[9] We reported a one-step synthesis of multicolor CDs from pyrolysis of epoxy-enriched polystyrene photonic crystals and their potential for use in light-emitting diodes.^[10] Herein, we present a simple and rapid strategy to fabricate CDs from cheap and natural carbon sources and further extend their application as printing “inks”.

The fluorescent CDs developed herein have the following notable characteristics: 1) one-step generation in minutes from low-cost, natural, edible chicken eggs by plasma-induced pyrolysis; 2) good amphiphilicity with high solubility in a broad range of aqueous and organic solvents; 3) resistance to acids and bases; 4) versatile applications as fluorescent carbon inks for luminescent patterns.

Figure 1 shows the fabrication of egg-derived fluorescent CDs and their application as “inks” for luminescent patterns using inkjet or silk-screen printing. We chose chicken eggs as the starting material to maintain low toxicity and affordability of the final product. Low-temperature plasma with high-

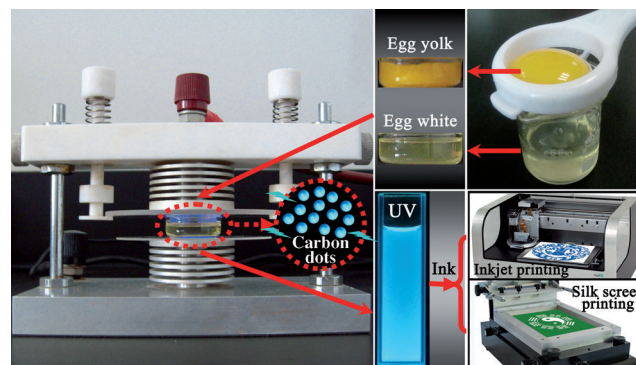


Figure 1. Digital photographs of plasma-induced fabrication of egg-derived CDs and their application as fluorescent carbon inks. Egg white or yolk, after a few minutes of plasma treatment under ambient conditions, were transformed into well-defined CDs with bright blue emission under UV light. The CD solutions can also be used as inks for making luminescent patterns by inkjet or silk-screen printing.

energy, inherently charged particles (electrons or cations) and excited neutral species was used to create an active chemical environment for the synthesis of the nanostructures.^[11] As shown in Figure 1, the egg was separated into egg white and egg yolk, using an egg-separator, prior to use. A glass dish filled with egg white or yolk was placed between two quartz slides (height = 1.5 cm) of the plasma generator. Subsequently, intense and uniform plasma beams generated from the upper electrode (voltage = 50 V, current = 2.4 A) irradiated the egg samples for 3 min to yield dark black products, referred to as CD_{pew} and CD_{pey} for the plasma-treated egg white and yolk, respectively. The yield of CDs from the egg sample was calculated to be approximately 5.96%. Elemental analysis showed an increase in the carbon content of the products (62.42% for CD_{pey} and 56.75% for CD_{pew}) in comparison to that of the starting material (57.55% for egg yolk and 43.50% for egg white), implying carbonization occurs during the plasma treatment (Supporting Information, Table S1). Significantly, solutions of CD_{pew} and CD_{pey} display bright blue fluorescence under UV light ($\lambda_{\text{ex}} = 302 \text{ nm}$).

Figure 2 shows high-resolution transmission electron microscope (HRTEM) images of the CDs. CD_{pey} had uniform dispersion without apparent aggregation and a mean particle diameter (D_p) of 2.15 nm (Figure 2a and Figure S2). Detectable rings in the selected-area electron-diffraction (SAED) pattern revealed the crystalline structure of CD_{pey} (Figure 2a inset). Well-resolved lattice fringes with an interplanar spacing of 0.208 nm were observed (Figure 2b), which is close to the (100) facet of graphite.^[1c,12] On the other hand, CD_{pew} was well distributed ($D_p = 3.39 \text{ nm}$) and appeared

[*] J. Wang, Dr. C.-F. Wang, Prof. S. Chen
State Key Laboratory of Materials-Oriented Chemical Engineering
and College of Chemistry and Chemical Engineering, Nanjing
University of Technology
Nanjing, 210009 (P.R. China)
E-mail: chensu@njut.edu.cn

[**] This work was supported by the National Natural Science Foundation of China (21076103), National Natural Science Foundation of China-NSAF (10976012), the Specialized Research Fund for the Doctoral Program of Higher Education of China (20093221120002, 20103221110001), the Priority Academic Program Development of Jiangsu Higher Education Institutions (PAPD), and National High Technology Research and Development Program of China (863 Program) (2012AA030313).

Supporting information for this article (experimental details) is available on the WWW under <http://dx.doi.org/10.1002/anie.201204381>.

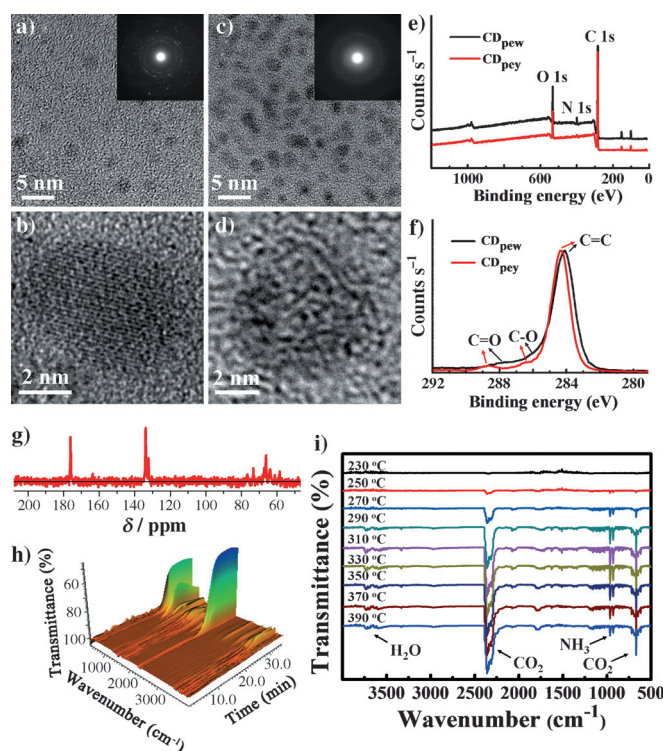


Figure 2. HRTEM images of CD_{ey} (a,b) and CD_{pew} (c,d) in aqueous solution, with an individual carbon dot at higher magnification (b,d). Inset: SAED patterns of the CDs. e) XPS spectra of CD_{pew} and CD_{ey} and f) the corresponding expansion of the C 1s peak. g) Solid-state ^{13}C NMR spectrum of CD_{ey} . h) Three-dimensional FTIR profile (40°C at 0 min to 390°C at 35 min) and i) the FTIR spectra (230–390°C) of the gases produced from egg white combustion.

amorphous in nature, as evidenced from the diffuse ring in the SAED pattern and the HRTEM image of an individual particle (Figure 2c,d). The difference in the morphologies of CD_{ey} and CD_{pew} might be explained by the higher lipid content in egg yolk (33%) than in egg white (0.01%; see Table S2). The lipids increase the density and viscosity of the egg yolk, which may enhance the residence time for the plasma to impose stronger electron-ion recombination on the sample surface, thus helping nanoparticle crystallization and shaping CD_{ey} into a crystalline form.^[13]

The chemical compositions and structures of the as-prepared CDs were investigated. X-ray photoelectron spectroscopy (XPS) of CD_{pew} and CD_{ey} showed the existence of carbon (C 1s, 284 eV), nitrogen (N 1s, 399 eV) and oxygen (O 1s, 532 eV; Figure 2e). In the expanded image of the C 1s peak (Figure 2f), the signals at 284.5 eV, 286.4 eV, and 288.6 eV demonstrate the presence of C=C, C–OH and C–O–C, and C=O functional groups,^[4a,14] which were further confirmed by FTIR spectroscopy (Figure S4).^[15] The solid-state ^{13}C NMR spectrum of CD_{ey} shows peaks at δ = 176.2 ppm (C=O), 133.8 ppm, 132.0 ppm (C=C), and 73.1 ppm and 66.2 ppm (C–OH; Figure 2g).^[16] An apparent G band at 1590 cm^{-1} and a weak D band at 1360 cm^{-1} were observed in the Raman spectrum of CD_{ey} (Figure S5), implying there are mainly sp^2 carbons with some sp^3 hybrid carbons in CD_{ey} . Therefore, we concluded that the egg-

derived CDs are mainly composed of sp^2 graphitic carbons with sp^3 carbon defects and abundant hydroxy and carbonyl/carboxylate groups at their surfaces.

To study the formation of egg-derived CDs, thermogravimetric analysis (TGA)/FTIR spectroscopy were used for the first time to record the pyrolysis procedure of egg white and CD_{pew} . As shown in Figure 2h, the egg white started to produce gases at approximately 230°C (19 min), generating a massive amount of CO_2 (2358 cm^{-1} and 669 cm^{-1}) along with less NH_3 (965 cm^{-1} and 931 cm^{-1}) and H_2O (3593 cm^{-1}) gases. We noticed that no gas was released from 40 to 230°C, which makes us hypothesize that the egg white may undergo complex reactions at this stage. As proposed in Figure S6, the high-temperature plasma initially gave powerful energy to pyrolyze albumens with nitrogen- and oxygen-containing functional groups, which was conducive to denaturing the protein through the breakage of hydrogen bonds and uncoiling of polypeptide chains.^[17] Meanwhile, the egg white reacted with the activated species in the plasma, leading to partial carbonization and oxidization of the sample. With continued plasma processing, the long and short chains of the peptides were further broken down into shorter chains and eventually CDs with abundant point effects.^[18] As seen in the FTIR spectra of egg white combusted from 230 to 390°C (Figure 2i), the CO_2 and NH_3 content gradually increased because of the combustion reaction of C and N atoms. This result resembled the pyrolysis process of CD_{pew} from 40 to 330°C (Figure S7) and demonstrated the formation of CD_{pew} after 230°C. The use of TGA/FTIR spectroscopy to record the formation of CDs is meaningful for other systems. Interestingly, this plasma-induced synthesis of fluorescent CDs can be extended to various precursors, like glucose, polyacrylamide, or amino acids (see details in Figure S9).

Figure 3 shows the optical properties of the egg-derived CDs. Both CD_{pew} and CD_{ey} exhibited an obvious absorption feature at approximately 275 nm in their UV/Vis absorption spectra. When excited at 360 nm, the CDs showed strong photoluminescence (PL) centered at approximately 420 nm, which gave blue fluorescence under UV light (Figure 3a). It is worth noting that the original egg sample was non-emissive under UV light; therefore, the luminescence arises from the nanoparticles, which have been shown to have radiative recombination of excitons at the particle surface.^[1a] The functional groups on the surface of the CDs might also be responsible for the PL emission.^[8c] The PL intensity of CD_{ey} appears higher than CD_{pew} , with their quantum yields determined to be 8% (CD_{ey}) and 6% (CD_{pew}) using quinine sulfate (54% in 0.5M sulfuric acid) as a reference. This variation is likely caused by more effective electronic transition in CD_{ey} . It has frequently been reported that the PL emission wavelength is dependent on the excitation, and we found the PL peaks of CD_{ey} in aqueous solution to be red-shifted from 420 nm to 560 nm by changing the excitation wavelength from 360 nm to 500 nm (Figure S11). Moreover, the PL intensities could be adjusted by the time of plasma treatment, in which gradually higher PL emission peaks were detected when the plasma treating intervals were increased from one minute to three minutes (Figure S12). Surprisingly, no obvious photobleaching was observed over a broad

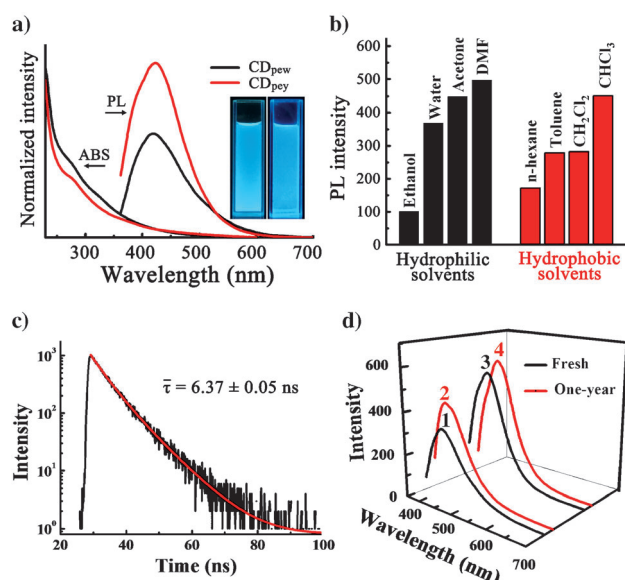


Figure 3. a) PL emission and UV/Vis absorption spectra of CD_{peg} and CD_{peg} in aqueous solution (λ_{ex} = 360 nm). Inset: digital photographs of CD_{peg} (left) and CD_{peg} (right) solutions under UV light. b) PL intensities of 1 wt% CD_{peg} in hydrophilic and hydrophobic solvents (λ_{ex} = 360 nm). c) A typical time-resolved fluorescence-decay curve of CD_{peg} (λ_{ex} = 405 nm) measured at 474 nm. d) PL spectra of fresh CD_{peg} and CD_{peg} after one year of storage (lines 1,2), and similar preparations of CD_{peg} (lines 3,4; λ_{ex} = 360 nm).

pH range of 1–14, demonstrating the good PL stability of CDs in different acidic/basic media (Figure S13).

These plasma-induced CDs are amphiphilic owing to the functional groups on their surfaces. As listed in Table S3, CD_{peg} has excellent solubility in water and various organic solvents (for example, 221 mg g⁻¹ in water and 665 mg g⁻¹ in DMF). As seen in the FTIR spectra (Figure S4), the relative absorption intensities for the –OH (3405 cm⁻¹), C–O (1262 cm⁻¹, 1118 cm⁻¹), and –COO⁻ (1664 cm⁻¹, 1384 cm⁻¹) groups on the CDs were higher than those of the starting materials, which may be related to the interaction between egg samples and the activated oxygen species (primarily O[•] and O[•]) produced by the plasma.^[19] Therefore, the use of plasma not only produces CDs from eggs in a simple manner, but also causes the formation of functional groups on the CD surface to give good solubility in a variety of solvents. We found that CD_{peg} showed different PL emission wavelengths and PL intensities in different hydrophobic and hydrophilic solvents (Figure 3b and Table S4). We believe that higher solubility of CD_{peg} in different solvents might be responsible for the stronger PL emission in both hydrophilic and hydrophobic solvents.

The fluorescence lifetime (τ) of CD_{peg} was assessed by time-resolved photoluminescence measurements. As seen in Figure 3c, the decay trace for CD_{peg} was fitted using biexponential functions $Y(t)$ based on non-linear least squares analysis in Equation (1).

$$Y(t) = a_1 \exp(-t/\tau_1) + a_2 \exp(-t/\tau_2) \quad (1)$$

where a_1 and a_2 are the fractional contributions of time-resolved decay lifetime of τ_1 and τ_2 .^[20] According to Equation (2),

$$\bar{\tau} = \frac{a_1 \tau_1^2 + a_2 \tau_2^2}{a_1 \tau_1 + a_2 \tau_2} \quad (2)$$

we calculated the average lifetime ($\bar{\tau}$) of CD_{peg} as 6.37 ± 0.05 ns ($\chi^2 < 1.1$), which was comparable to reported values.^[21] Moreover, these CDs exhibited favorable photostability with approximately 10 % improvement in their PL intensities after storage for one year under ambient conditions (Figure 3d).

Finally, we applied these CDs as fluorescent carbon inks for printing versatile fluorescent patterns. Inkjet printing is a useful technique for creating highly-defined patterns, which can be used for conductive circuits, flexible electronics, and fingerprint recognition, for example.^[22] So far, single-walled carbon nanotubes, luminescent CdTe nanocrystals/polymer composites, and fluorescein have been patterned using this method.^[23] Whereas, to our knowledge, the use of CDs for versatile patterns still remains rare. Figure 4a shows the inkjet

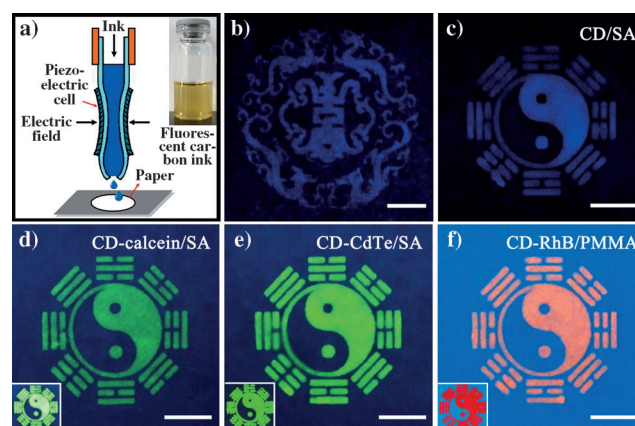


Figure 4. a) Scheme of piezoelectric inkjet printing. Inset: the as-prepared fluorescent carbon ink. b) Photograph of the fluorescent pattern representing blue and white porcelain by inkjet printing. Photographs of fluorescent Tai Chi patterns by silk-screen printing from different mixtures of CDs: c) CD/SA, d) CD-calcein/SA, e) CD-CdTe/SA, and f) CD-RhB/PMMA under UV light. Scale bar = 1 cm. Insets of (d), (e) and (f) are photographs of patterns from calcein/SA, CdTe/SA, and RhB/PMMA mixtures, respectively, under UV light for comparison.

printing process; the piezoelectric materials change their shape when an electric field is applied, which generates a pressure pulse, and actuates the connecting pump to inject ink droplets out of the nozzle. We prepared a printable fluorescent ink by blending CD_{peg} with glycol, a benign humectant that helps prevent the nozzle from clogging. The optimal surface tension and viscosity (the two most important factors of inks) were determined to be 44.0 mN m⁻¹ and 3.51 cP, respectively, after several trials. Additionally, this CD/glycol mixture has high electrical conductivity (6.76 S m⁻¹), making it promising for optoelectronic devices. The CD/

glycol mixture was printed using a Dimatix DMP 2831 printer, a fluorescent image of blue and white porcelain was formed on the paper substrate in 20 minutes (Figure 4b). Moreover, a cheaper and simpler method, silk-screen printing (with promise for applications such as solar cells),^[24] was also used for making fluorescent patterns. We chose sodium alginate (SA) as a matrix owing to its benign affinity to the CDs (Figure S14). The CD/SA ink was screened through woven meshes onto a paper substrate by extrusion using a scraper blade, and was transferred as a bright blue-emitting “Tai Chi” pattern (Figure 4c). Furthermore, this fluorescent ink can also be used with the pen-on-paper technique,^[25] a unique approach for the fabrication of flexible devices (Figure S15).

To expand the CD patterns beyond a single fluorescent color in the patterns, we tuned the PL emissions by doping CD_{pey} with a small amount of organic dye or semiconductor QDs in the water- or oil-phases owing to the amphiphilic nature of the CDs. A series of homogeneous and transparent solutions were prepared by blending CD/SA aqueous solutions with calcein ($\lambda_{\text{em}} = 534$ nm) and CdTe QDs ($\lambda_{\text{em}} = 562$ nm) and by mixing a chloroform solution of CD_{pey} with rhodamine B (RhB) ($\lambda_{\text{em}} = 615$ nm) in a poly(methyl methacrylate) (PMMA) matrix. The PL spectra of these composites showed two emission peaks, assigned to the characteristic emissions of CD_{pey} ($\lambda_{\text{em}} = 430$ nm) and the introduced fluorescent materials, that is, calcein, CdTe QDs, or RhB (the longer wavelength emission, shown in Figure S16), which indicates that the mixture contains the properties of both fluorescent components. Moreover, as the concentration of the fluorescent material increases, the PL intensity gradually increases, while the PL intensity of the CDs simultaneously undergoes some fluorescence quenching. This result implies that fluorescence resonance energy transfer (FRET) from CDs to the introduced materials may occur in these systems.^[26] Because the PL emission spectra of CDs overlap with the absorption spectra of calcein (400–455 nm), CdTe QDs (380–525 nm) and RhB (455–500 nm), the CDs can act as a donor and non-radiatively transfer their excitation energy to the proximal molecules of the fluorescent materials (the FRET acceptor), thereby resulting in the changes in the PL intensities and emission peaks of both components. In Figure 4d–f, at a typical weight ratio of calcein, CdTe QDs, or RhB to CDs of 0.0375, we obtained bluish-green, yellowish-green, and pink Tai Chi patterns from these composite solutions, respectively, which are different from the green, verdure, and red colors of pure calcein/SA, CdTe/SA, or RhB/PMMA solutions. This suggests that the combination of CDs with an appropriate fluorescent material allows for the manipulation of photoluminescence for multicolor patterns.

In summary, we have described a rapid plasma-induced method for accessing fluorescently stable carbon dots (CDs) using cheap and natural chicken eggs as the precursor. The plasma treatment offers amphiphilicity to the CDs, making them dispersible in water and most organic solvents. A possible mechanism for egg-derived CD formation has been proposed from the results of FTIR spectroscopy on evolved gases during the pyrolysis process. We have extended the use of CDs as fluorescent inks for multicolor patterns using inkjet and silk-screen printing, which may be useful in optoelec-

tronic fields. This method can be used to produce CDs from a wide range carbon sources for many different applications.

Received: June 6, 2012

Revised: July 19, 2012

Published online: August 21, 2012

Keywords: carbon dots · inkjet printing · photoluminescence · plasma chemistry · quantum dots

- [1] a) Y.-P. Sun, B. Zhou, Y. Lin, W. Wang, K. A. S. Fernando, P. Pathak, M. J. Meziani, B. A. Harruff, X. Wang, H. Wang, P. G. Luo, H. Yang, M. E. Kose, B. Chen, L. M. Veca, S.-Y. Xie, *J. Am. Chem. Soc.* **2006**, *128*, 7756–7757; b) L. Zheng, Y. Chi, Y. Dong, J. Lin, B. Wang, *J. Am. Chem. Soc.* **2009**, *131*, 4564–4565; c) S. N. Baker, G. A. Baker, *Angew. Chem.* **2010**, *122*, 6876–6896; *Angew. Chem. Int. Ed.* **2010**, *49*, 6726–6744; d) Q. Li, T. Y. Ohulchanskyy, R. Liu, K. Koynov, D. Wu, A. Best, R. Kumar, A. Bonoio, P. N. Prasad, *J. Phys. Chem. C* **2010**, *114*, 12062–12068; e) S.-T. Yang, X. Wang, H. Wang, F. Lu, P. G. Luo, L. Cao, M. J. Meziani, J.-H. Liu, Y. Liu, M. Chen, Y. Huang, Y.-P. Sun, *J. Phys. Chem. C* **2009**, *113*, 18110–18114.
- [2] a) L. Cao, X. Wang, M. J. Meziani, F. Lu, H. Wang, P. G. Luo, Y. Lin, B. A. Harruff, L. M. Veca, D. Murray, S.-Y. Xie, Y.-P. Sun, *J. Am. Chem. Soc.* **2007**, *129*, 11318–11319; b) S.-T. Yang, L. Cao, P. G. Luo, F. Lu, X. Wang, H. Wang, M. J. Meziani, Y. Liu, G. Qi, Y.-P. Sun, *J. Am. Chem. Soc.* **2009**, *131*, 11308–11309; c) H. Li, X. He, Z. Kang, H. Huang, Y. Liu, J. Liu, S. Lian, C. H. A. Tsang, X. Yang, S.-T. Lee, *Angew. Chem.* **2010**, *122*, 4532–4536; d) H. Gonçalves, P. A. S. Jorge, J. R. A. Fernandes, J. C. G. E. da Silva, *Sens. Actuators B* **2010**, *145*, 702–707; e) F. Wang, Y. Chen, C. Liu, D. Ma, *Chem. Commun.* **2011**, *47*, 3502–3504; f) H. X. Zhao, L. Q. Liu, Z. D. Liu, Y. Wang, X. J. Zhao, C. Z. Huang, *Chem. Commun.* **2011**, *47*, 2604–2606; g) Y.-P. Sun, X. Wang, F. Lu, L. Cao, M. J. Meziani, P. G. Luo, L. Gu, L. M. Veca, *J. Phys. Chem. C* **2008**, *112*, 18295–18298.
- [3] a) X. Li, H. Wang, Y. Shimizu, A. Pyatenko, K. Kawaguchi, N. Koshizaki, *Chem. Commun.* **2011**, *47*, 932–934; b) Q.-L. Zhao, Z.-L. Zhang, B.-H. Huang, J. Peng, M. Zhang, D.-W. Pang, *Chem. Commun.* **2008**, 5116–5118; c) X. Wang, K. Qu, B. Xu, J. Ren, X. Qu, *J. Mater. Chem.* **2011**, *21*, 2445–2450; d) Z.-A. Qiao, Y. Wang, Y. Gao, H. Li, T. Dai, Y. Liu, Q. Huo, *Chem. Commun.* **2010**, *46*, 8812–8814; e) A. B. Bourlinos, A. Stassinopoulos, D. Anglos, R. Zboril, V. Georgakilas, E. P. Giannelis, *Chem. Mater.* **2008**, *20*, 4539–4541; f) A. B. Bourlinos, R. Zboril, J. Petr, A. Bakandritsos, M. Krysmann, E. P. Giannelis, *Chem. Mater.* **2012**, *24*, 6–8.
- [4] a) D. Pan, J. Zhang, Z. Li, M. Wu, *Adv. Mater.* **2010**, *22*, 734–738; b) J. Shen, Y. Zhu, C. Chen, X. Yang, C. Li, *Chem. Commun.* **2011**, *47*, 2580–2582.
- [5] J. Zhou, C. Booker, R. Li, X. Zhou, T.-K. Sham, X. Sun, Z. Ding, *J. Am. Chem. Soc.* **2007**, *129*, 744–745.
- [6] A. B. Bourlinos, A. Stassinopoulos, D. Anglos, R. Zboril, M. Karakassides, E. P. Giannelis, *Small* **2008**, *4*, 455–458.
- [7] D. Pan, J. Zhang, Z. Li, C. Wu, X. Yan, M. Wu, *Chem. Commun.* **2010**, *46*, 3681–3683.
- [8] a) R. Liu, D. Wu, S. Liu, K. Koynov, W. Knoll, Q. Li, *Angew. Chem.* **2009**, *121*, 4668–4671; *Angew. Chem. Int. Ed.* **2009**, *48*, 4598–4601; b) H. Liu, T. Ye, C. Mao, *Angew. Chem.* **2007**, *119*, 6593–6595; *Angew. Chem. Int. Ed.* **2007**, *46*, 6473–6475; c) S.-L. Hu, K.-Y. Niu, J. Sun, J. Yang, N.-Q. Zhao, X.-W. Du, *J. Mater. Chem.* **2009**, *19*, 484–488; d) X. Wang, L. Cao, F. Lu, M. J. Meziani, H. Li, G. Qi, B. Zhou, B. A. Harruff, F. Kermarrec, Y.-P. Sun, *Chem. Commun.* **2009**, 3774–3776; e) H. Peng, J. Travas-Sejdic, *Chem. Mater.* **2009**, *21*, 5563–5565.

- [9] a) F. Wang, S. Pang, L. Wang, Q. Li, M. Kreiter, C. Liu, *Chem. Mater.* **2010**, *22*, 4528–4530; b) H. Zhu, X. Wang, Y. Li, Z. Wang, F. Yang, X. Yang, *Chem. Commun.* **2009**, 5118–5120.
- [10] X. Guo, C.-F. Wang, Z.-Y. Yu, L. Chen, S. Chen, *Chem. Commun.* **2012**, *48*, 2692–2694.
- [11] a) J. Zheng, R. Yang, L. Xie, J. Qu, Y. Liu, X. Li, *Adv. Mater.* **2010**, *22*, 1451–1473; b) F. Liu, P. Cao, H. Zhang, J. Tian, C. Xiao, C. Shen, J. Li, H. Gao, *Adv. Mater.* **2005**, *17*, 1893–1897.
- [12] Y. Dong, N. Zhou, X. Lin, J. Lin, Y. Chi, G. Chen, *Chem. Mater.* **2010**, *22*, 5895–5899.
- [13] L. Mangolini, E. Thimsen, U. Kortshagen, *Nano Lett.* **2005**, *5*, 655–659.
- [14] a) S. N. Jampala, M. Sarmadi, E. B. Somers, A. C. L. Wong, F. S. Denes, *Langmuir* **2008**, *24*, 8583–8591; b) Y. Fan, H. Cheng, C. Zhou, X. Xie, Y. Liu, L. Dai, J. Zhang, L. Qu, *Nanoscale* **2012**, *4*, 1776–1781; c) S. C. Ray, A. Saha, N. R. Jana, R. Sarkar, *J. Phys. Chem. C* **2009**, *113*, 18546–18551.
- [15] a) L. Tian, D. Ghosh, W. Chen, S. Pradhan, X. Chang, S. Chen, *Chem. Mater.* **2009**, *21*, 2803–2809; b) L. Hou, L. Chen, S. Chen, *Langmuir* **2009**, *25*, 2869–2874; c) Y.-K. Chen, Y.-F. Lin, Z.-W. Peng, J.-L. Lin, *J. Phys. Chem. C* **2010**, *114*, 17720–17727.
- [16] M. J. Krysmann, A. Kelarakis, P. Dallas, E. P. Giannelis, *J. Am. Chem. Soc.* **2012**, *134*, 747–750.
- [17] Y. Mine, *Trends Food Sci. Technol.* **1995**, *6*, 225–232.
- [18] H. Jiang, F. Chen, M. G. Lagally, F. S. Denes, *Langmuir* **2010**, *26*, 1991–1995.
- [19] a) B. Balu, V. Breedveld, D. W. Hess, *Langmuir* **2008**, *24*, 4785–4790; b) H. Li, C.-S. Ha, I. Kim, *Langmuir* **2008**, *24*, 10552–10556.
- [20] a) H. Zhong, Y. Zhou, M. Ye, Y. He, J. Ye, C. He, C. Yang, Y. Li, *Chem. Mater.* **2008**, *20*, 6434–6443; b) S. Yang, C.-F. Wang, S. Chen, *J. Am. Chem. Soc.* **2011**, *133*, 8412–8415.
- [21] A. Jaiswal, S. S. Ghosh, A. Chattopadhyay, *Chem. Commun.* **2012**, *48*, 407–409.
- [22] a) H. Sirringhaus, T. Kawase, R. H. Friend, T. Shimoda, M. Inbasekaran, W. Wu, E. P. Woo, *Science* **2000**, *290*, 2123–2126; b) Y. Yoshioka, G. E. Jabbour, *Adv. Mater.* **2006**, *18*, 1307–1312.
- [23] a) K. Kordás, T. Mustonen, G. Tóth, H. Jantunen, M. Lajunen, C. Soldano, S. Talapatra, S. Kar, R. Vajtai, P. M. Ajayan, *Small* **2006**, *2*, 1021–1025; b) E. Tekin, P. J. Smith, S. Hoepfner, A. M. J. van den Berg, A. S. Susha, A. L. Rogach, J. Feldmann, U. S. Schubert, *Adv. Funct. Mater.* **2007**, *17*, 23–28; c) S. Yang, C.-F. Wang, S. Chen, *Angew. Chem.* **2011**, *123*, 3790–3793; *Angew. Chem. Int. Ed.* **2011**, *50*, 3706–3709.
- [24] F. C. Krebs, M. Jørgensen, K. Norrman, O. Hagemann, J. Alstrup, T. D. Nielsen, J. Fyenbo, K. Larsen, J. Kristensen, *Sol. Energy Mater. Sol. Cells* **2009**, *93*, 422–441.
- [25] A. Russo, B. Y. Ahn, J. J. Adams, E. B. Duoss, J. T. Bernhard, J. A. Lewis, *Adv. Mater.* **2011**, *23*, 3426–3430.
- [26] a) K. J. Lee, J. H. Oh, Y. Kim, J. Jang, *Adv. Mater.* **2006**, *18*, 2216–2219; b) Y. Ner, J. G. Grote, J. A. Stuart, G. A. Sotzing, *Angew. Chem.* **2009**, *121*, 5236–5240; *Angew. Chem. Int. Ed.* **2009**, *48*, 5134–5138; c) I. L. Medintz, A. R. Clapp, J. S. Melinger, J. R. Deschamps, H. Mattoussi, *Adv. Mater.* **2005**, *17*, 2450–2455; d) A. R. Clapp, I. L. Medintz, J. M. Mauro, B. R. Fisher, M. G. Bawendi, H. Mattoussi, *J. Am. Chem. Soc.* **2004**, *126*, 301–310; e) A. M. Dennis, G. Bao, *Nano Lett.* **2008**, *8*, 1439–1445; f) H. Duan, M. Kuang, Y. A. Wang, *Chem. Mater.* **2010**, *22*, 4372–4378.